E3S Web of Conferences **152**, 03010 (2020) https://doi.org/10.1051/e3sconf/202015203010
PEEE 2019

Analysis of the effect neutral connection mode for permanent magnet synchronous generator-vienna rectifier set

Mohamed Amine Bettouche[1,2*], *Mohamed Fouad* Benkhoris[1], *Jean-Claude* Le Claire[1], *Djamal* Aouzellag[2], *Kaci* Ghedamsi[2], and *Mourad* Ait Ahmed[1]

[1]IREENA - Laboratory, University of Nantes 44602, Saint-Nazaire, France
[2]LMER - Laboratory, University of Bejaia 06000- Bejaia – Algeria

Abstract. In this paper, it was considered to investigate a new electrical architecture for the conversion of mechanical energy from renewable sources into electrical energy, fault tolerant and high energy and dynamic performance for the exploitation of marine renewable energy (MRE). The architecture to be investigated concerns a three-phase permanent magnet synchronous generator combined with a Vienna rectifier, with a topology that minimizes the number of active switches to increase the reliability of the energy conversion chain. Despite the high non-linearity of this architecture, this control is made possible through to the dynamic performance and control of the maximum switching frequency of the self-oscillating controller called the Phase-Shift Self-Oscillating Current-Controller (PSSOCC). The study of the impact of the connection of the PMSG neutral to the mid-point of the DC bus is being investigated.

1 Introduction

Marine energy is one of the most interesting emerging form of renewable energy. Tidal turbines are used to extract this energy and installed on the seabed, permanent-magnet synchronous generators (PMSG) are common in this case due to their efficiency and high-power density. The PMSG can be associated with an PWM rectifier or with a three-phase diode rectifier [1-3]. In this paper the PMSG is combining with a three-phase rectifier of the Vienna type [4–6]. This new fault tolerant conversion architecture is of particular interest in the case of the exploitation of marine renewable energies where access to facilities is difficult. However, this topology is highly non-linear. The establishment of the equivalent continuous dynamic model is not easy. The regulation of the currents constituting the internal loops is ensured by a phase-shift self-oscillating current-controller (PSSOCC). In this paper, after presenting the architecture of the complete energy conversion chain, we recall the PMSG model in the natural base, then we explain the current control strategy and describe in a synthetic way the PSSOCC. Then we are interested in the study of the impact of the connection or not of the neutral point of the PMSG to the mid-point of the DC bus, on the time behavior of the chain of the PMSG-rectifier association Vienna.

2 Description of the energy conversion chain

Figure 1. shows the complete chain of conversion of energy from marine currents into electrical energy. The PMSG is a 500 kW. Compared to the PWM rectifier, the Vienna rectifier has only 3 IGBTs instead of 6, which reduces the number of active switches and improves the reliability of the AC-DC power conversion stage. The inverter allows the conversion of DC-AC electrical energy to grid frequency. The Vienna control signals are generated by the three-phase PSSOCC that controls the PMSG phase currents and the PWM function.

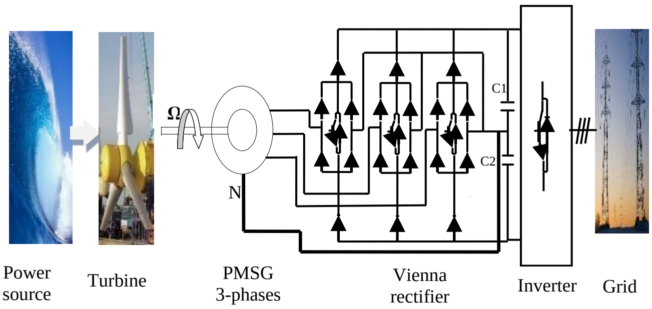

Fig. 1. Architecture of the energy conversion chain

Subsequently, the study focuses on the PMSG-Vienna rectifier association. The part concerning the connection to the network is modelled by a variable resistance. In this study we assume that variation of the speed marine currents is low and that the PMSG speed is assumed to be constant and equal to 272.7 rpm, with a frequency of 50Hz.

3 Dynamic model of the PMSG

The permanent magnet synchronous generator with smooth poles and a sinusoidal distribution. the phenomenon of saturation, effect of temperature and iron

*Corresponding author: mohamed-amine.bettouche@etu.univ-nantes.fr

losses are neglected. The expression of stator voltages is given by the following relationship:

$$[V_s] = [R_s].[i_s] + \frac{d\,[\emptyset_s]}{dt} \quad (1)$$

Where:

$$[V_s] = [V_{as}\;\; V_{bs}\;\;\; V_{cs}]^T \quad (2)$$

$$[i_s] = [i_a\; i_b\;\;\; i_c]^T \quad (3)$$

$$[R_s] = diag[R_a\, R_b\, R_c] \quad (4)$$

$$[\phi_s] = [\phi_{as}\;\; \phi_{bs}\;\;\; \phi_{cs}]^T \quad (5)$$

The expression of magnetic flux is given by:

$$[\emptyset_s] = [M].[i_s] + \Psi.[F_s] \quad (6)$$

With:

$$[F_s] = \begin{bmatrix} cos(P\theta) \\ cos(P\theta - \frac{2.\pi}{3}) \\ cos(P\theta + \frac{2.\pi}{3}) \end{bmatrix} \quad (7)$$

The electrical equations of the PMSG in the natural base, are written in matrix form:

$$\begin{bmatrix} V_a \\ V_b \\ V_c \end{bmatrix} = \begin{bmatrix} E_a \\ E_b \\ E_c \end{bmatrix} - R_s \begin{bmatrix} I_a \\ I_b \\ I_c \end{bmatrix} - \begin{bmatrix} (l_f + M_s) & M_s.cos(\frac{2\pi}{3}) & M_s.cos(-\frac{2\pi}{3}) \\ M_s.cos(-\frac{2\pi}{3}) & (l_f + M_s) & M_s.cos(\frac{2\pi}{3}) \\ M_s.cos(\frac{2\pi}{3}) & M_s.cos(-\frac{2\pi}{3}) & (l_f + M_s) \end{bmatrix} \frac{d}{dt} \begin{bmatrix} I_a \\ I_b \\ I_c \end{bmatrix} \quad (8)$$

$$\begin{bmatrix} E_a \\ E_b \\ E_c \end{bmatrix} = \Psi.\Omega.P.\begin{bmatrix} cos(\theta) \\ cos(\theta - \frac{2.\pi}{3}) \\ cos(\theta + \frac{2.\pi}{3}) \end{bmatrix} \quad (9)$$

Where: Ψ is the flux of permanent magnets and P is the number of pole pairs.

The voltage equations of the PMSG for each phase are:

$$V_a = E_a - R_s i_a - (l_f + M_s)\frac{dia}{dt} + \frac{M_s\,dib}{2\;\;dt} + \frac{M_s\,dic}{2\;\;dt} \quad (10)$$

$$V_b = E_b - R_s i_b - (l_f + M_s)\frac{dib}{dt} + \frac{M_s\,dia}{2\;\;dt} + \frac{M_s\,dic}{2\;\;dt} \quad (11)$$

$$V_c = E_c - R_s i_c - (l_f + M_s)\frac{dic}{dt} + \frac{M_s\,dia}{2\;\;dt} + \frac{M_s\,dib}{2\;\;dt} \quad (12)$$

In the case of the neutral of PMSG is connected to the DC bus, (Figure 2.), we have: $i_a + i_b + i_c = i_N$ (13)

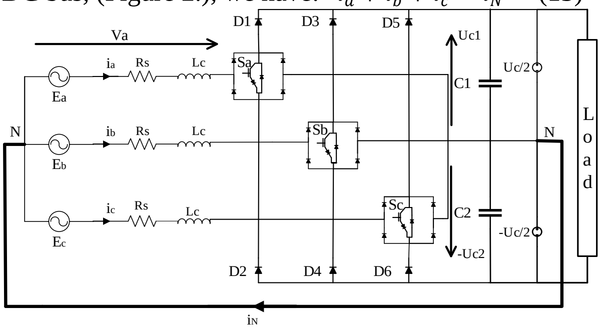

Fig. 2. PMSG-Vienna rectifier, neutral connected

By summing equations (10), (11), (12), we can easily deduce:

$$V_a + V_b + V_c = -R_s\, i_N - l_f\, \frac{di_N}{dt} \quad (14)$$

The phase voltage can be expressed as a function of the phase current (i_a) and the current in the neutral (i_N), we obtain:

$$V_a = E_a - R_s i_a - L_c \frac{dia}{dt} + \frac{M_s\, di_N}{2\, dt} \quad (15)$$

Where: $L_c = l_f + \frac{3M_s}{2}$ (16)

In the case of the neutral of PMSG is not connected to the DC bus (neutral floating), (Figure 3.), we have:

$$i_a + i_b + i_c = 0 \quad (17)$$

The phase voltage become: $V_a = E_a - R_s i_a - L_c \frac{dia}{dt}$ (18)

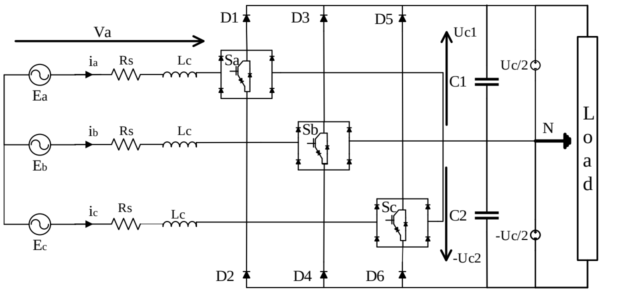

Fig. 3. PMSG-Vienna rectifier, neutral not connected (floating)

4 Control strategy and current regulation

In this study, the generator currents are controlled in the ABC frame. To achieve the objective of collinearity of the current and emf vectors, the emf must be previously tabulated or estimated in real time on the one hand, and the reference of the current vector must be in phase with the emf vector on the other hand.

The tracking of current references is ensured by the PSSOCC [7-8] whose performances have been shown through many applications using static converters integrated in electrical energy conversion chains [9-10], speed variators, active filters, sinusoidal absorption converters... The PSSOCC is a self-oscillating regulator, of analog type with very high dynamics (very wide bandwidth). Its advantages include maximum switching frequency control, very low sensitivity to system parameters and good stability and low THD in the currents. Its principle involves two basic functions: the regulation of the current by low frequencies and the control of the switching frequency in high frequencies. Sound complete study was done in [11]. Figure 4. shows the basic synoptic of the PSSOCC.

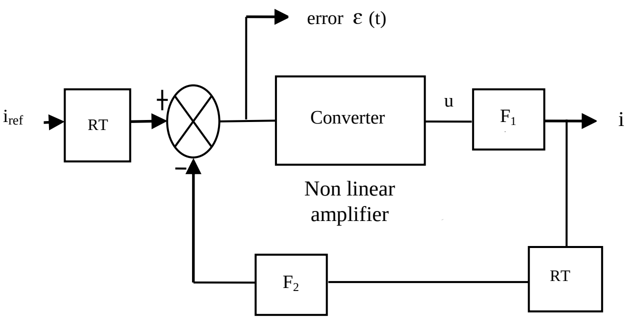

Fig. 4. Basic overview of the self-oscillating controller

The transfer functions F1(p), F2(p) and RT represent respectively the "voltage-current" transfer function of the load, the transfer function of a second-order low-pass filter and the transfer function of the current sensor. The status of the converter depends on the error *ε(t)*. If the error *ε(t)* is positive, the output of the converter *u(t)* is positive. If the error *ε(t)* is negative, the output *u(t)* of the converter is negative. The filter F2 is calculated in such a way that the system voluntarily oscillates. The oscillation frequency obtained represents the maximum switching frequency. It has been shown that the system oscillates when a phase rotation of *-180°* is introduced by filters F1(p) and F2(p). The natural frequency f0 of the filter F2 is higher than the cut-off frequency of the filter F1 so that at the oscillation frequency, the phase shift introduced by the latter is almost equal to *-90°*. At the oscillation frequency the phase shift introduced by the F2 filter is also close to *-90°*. The error detector introduces a *180°* phase rotation on the signal at the output of the filter F2. Therefore, the phase shift introduced by the error detector and filters assembly is zero.

5 Study the impact of the connection of the PMSG neutral and the mid-point of the DC bus

Two cases were investigated according to the PMSG neutral connection mode (Figures (5., 13.)). The entire inverter-grid is modelled by a variable resistive load.

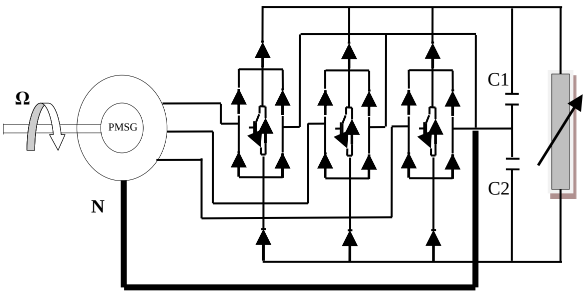

Fig. 5. Neutral connected

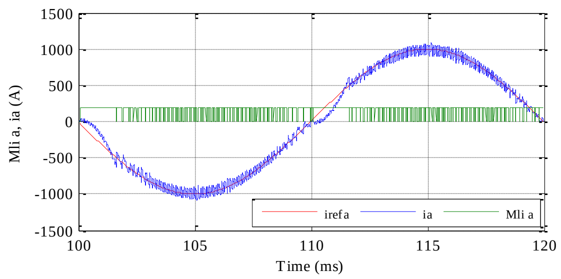

Fig. 6. Current phase one, MLI signal (Neutral connected)

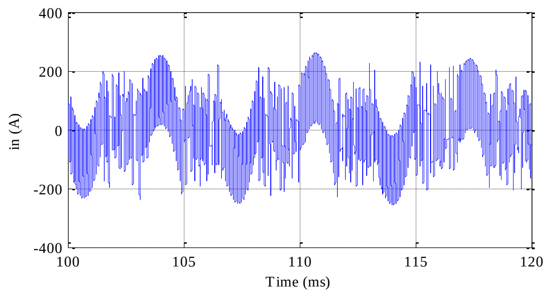

Fig. 7. Current in neutral (Neutral connected)

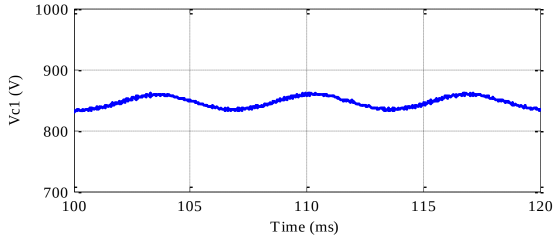

Fig. 8. Voltage Vc1 (Neutral connected)

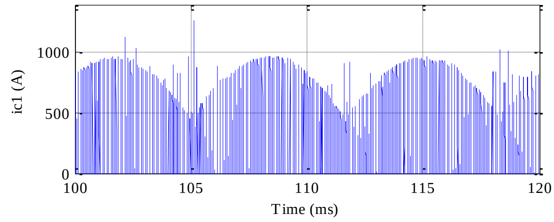

Fig. 9. Current ic1 (Neutral connected)

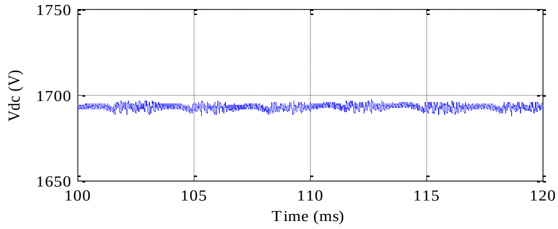

Fig. 10. Voltage Vdc (Neutral connected)

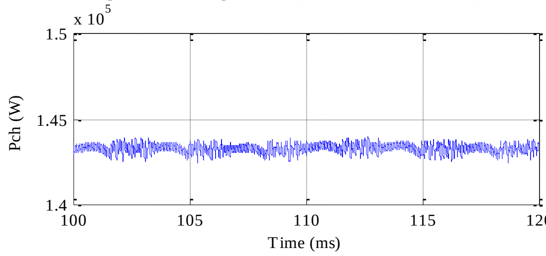

Fig. 11. Power at the load terminal (Neutral connected)

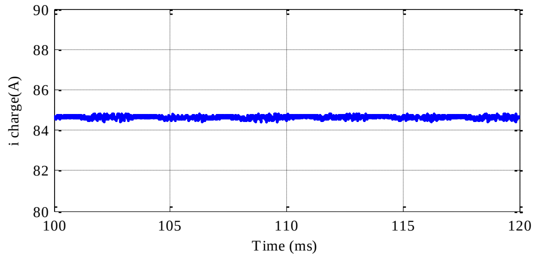

Fig. 12. Current at the load terminal (Neutral connected)

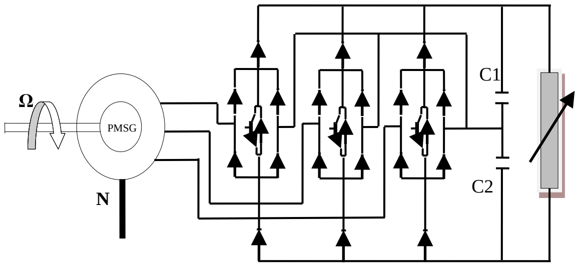

Fig. 13. Neutral not connected (floating)

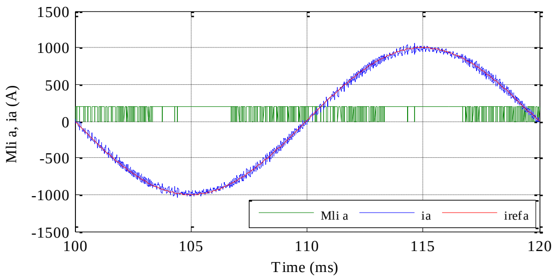

Fig. 14. Current phase one, MLI signal (neutral floating)

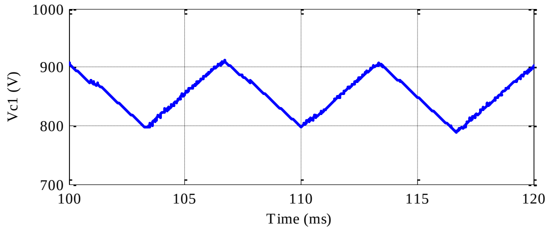

Fig. 15. Voltage Vc1 (neutral floating)

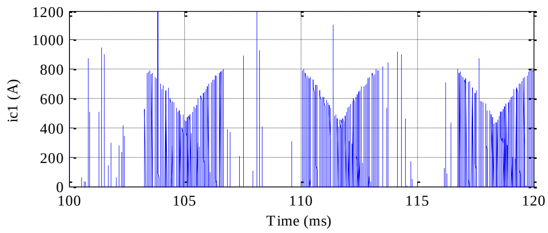

Fig. 16. Current ic1 (neutral floating)

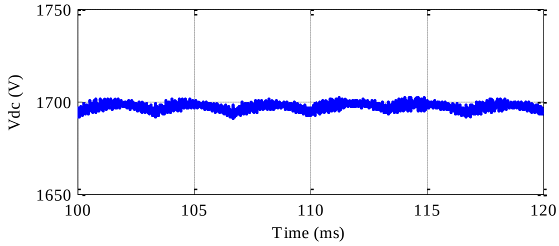

Fig. 17. Voltage Vdc (neutral floating)

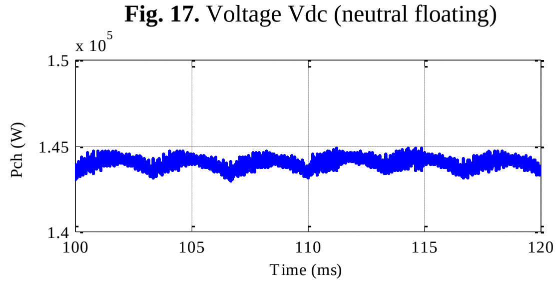

Fig. 18. Power at the load terminal (neutral floating)

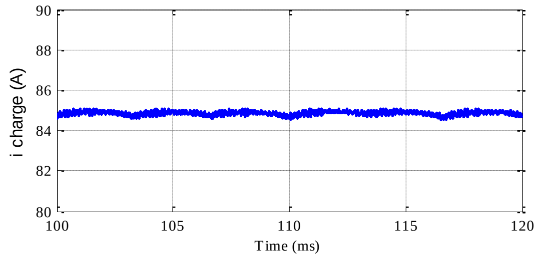

Fig. 19. Current at the load terminal (neutral floating)

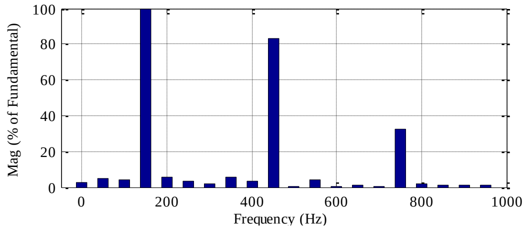

Fig. 20. Harmonic analysis of the current in the neutral

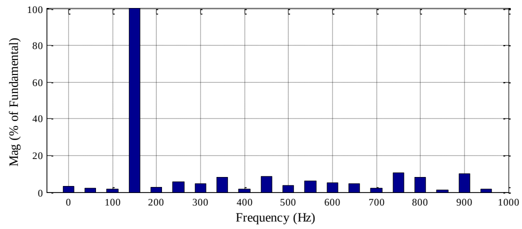

Fig. 21. Harmonic analysis of the current ic1 (Neutral connected)

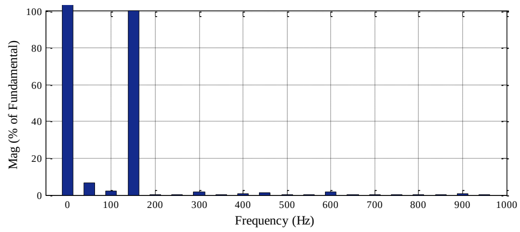

Fig. 22. Harmonic analysis of the voltage Vc1 (Neutral connected)

The simulations were performed using Matlab/Simulink software. Figure 14. represents the phase current of the machine for the case neutral floating, the regulators (PSSOCC) ensure a good tracking of the current references within the physical limit of the system. Indeed, when the reference current passes through zero, the (PSSOCC) maintains the control signal of the ON switch so that the measured current reaches its reference. If the neutral is connected, the zero-sequence current and multiples of 3 exist as shown by the harmonic analysis of the phase current. In the case of the neutral connected to the DC bus (Figure 6.), the phase current is disconnected from its reference at zero crossings, which is related to the structure of the Vienna and the instantaneous values of the emf.

Figure 7. represents the current flowing in the neutral. We notice that it is at a frequency of (3*f) compared to the fundamental, which is due to the appearance of harmonic 3 and its multiples (Figure 20.).

The way the neutral is connected to an influence on the voltages of both capacitors (C1 and C2), or in the case of the floating neutral (Figure 15.), generates undulations of the voltage V_{c1}, which is not the case when the neutral is connected (Figure 8.).

Figures 10. and Fig. 17. show the DC bus voltage for both cases of the neutral connection mode, we can see that there is a small difference between the two values, the difference is due to the effect of mutual inductance between the different phases. Figures 11. and 18.

represent respectively the power at the load terminal for the both cases, the same thing is noticed with the case of the two voltages.

The currents at the load terminal for both cases are illustrated in the Figures 12. and Fig. 19., and the Figures (9., 16.) represent the current i_{c1} at the capacitor (C1) for the both cases of neutral connection mode.

The harmonic analysis of the current and the voltage at the capacitor terminal for the case of the neutral connected shows the appearance of the harmonic 3 (Figures 21., 22.).

The deformation of the current induces harmonics, which are given in the following tables:

Table 1. Harmonic distortion coefficient in the current phase of the Vienna neutral connected

Converter	Vienna: neutral connected with the mid-point of the DC bus			
Harmonic rank	3	5	7	9
(%) of the fundamental	2.30	2.25	2.09	1.79

Table 2. Harmonic distortion coefficient in the current phase of the Vienna neutral not connected

Converter	Vienna: neutral not connected with the mid-point of the DC bus (floating neutral)			
Harmonic rank	3	5	7	9
(%) of the fundamental	0	0.29	0.18	0

Table 3. Parameters of the machine

Number of pole pairs	p	11
Phase Resistance	R_s (ohm)	6.3060*10$^{(-4)}$
Leakage inductance	L_f (H)	3.0918*10$^{(-5)}$
Mutual inductance	M_s (H)	2.2848*10$^{(-5)}$
Capacitor	$C_1 = C_2$ (mF)	2200
Maximum flow	Ψ_{max} (Wb)	0.3244

6. Conclusion

Despite the high non-linearity of the architecture studied, through the use of the PSSOCC, the currents of PMSG follow the references optimizing energy conversion within the physical limits of the system. The simulations conducted show the impact of the connection of the neutral to the mid-point of the DC bus on the quality of the phase currents and DC bus voltages.

References

1. Z. Qiu, K. Zhou, and Y. Li "*Modeling and control of diode rectifier fed PMSG based wind turbine*", 4th International Conference on Electric Utility Deregulation and Restructuring and Power Technologies, Shandong, China, 6-9 July 2011.
2. M.F. Iacchetti, G.M. Foglia, A.Di Gerlando, and A.J. Forsyth "*Analytical Evaluation of Surface-Mounted PMSG Performances Connected to a Diode Rectifier*", IEEE Transactions on Energy Conversion, Vol. 30, pp. 1367 – 1375, July 2015.
3. P. Chimurkar, and P. Kothavade "*Simulation of Modified Rectifier System for Variable Speed High Power PMSG Wind Turbine by using Filter*", International Conference on Current Trends in Computer, Electrical, Electronics and Communication, Mysore, India, 8-9 September 2017.
4. J.S. Lee, and K.Beum. Lee "*Predictive Control of Vienna Rectifiers for PMSG Systems*", IEEE Transactions on Industrial Electronics, Vol. 64, pp 2580 – 2591, April 2017.
5. J.S. Lee, Y. Bak, K.B Lee, and F. Blaabjerg "*MPC-SVM method for Vienna rectifier with PMSG used in Wind Turbine Systems*", IEEE Applied Power Electronics Conference and Exposition, CA, USA, 20-24 March 2016.
6. A. Rajaei, M. Mohamadian, and A.Y. Varjani "*Vienna-Rectifier-Based Direct Torque Control of PMSG for Wind Energy Application*", IEEE Transactions on Industrial Electronics, Vol. 60, pp. 2919 – 2929, July 2013.
7. J.C. Le Claire, "*Circuits spécifiques pour commande de machines à courants lternatifs*", PhD thesis, University of Nantes, January 1999.
8. J.C. Le Claire, S. Siala, J. Saillard, and R. Le Doeuff, "*Method and device for controlling switches in a control system with variable structure, with controllable frequency*", US patent n° 6.376.935 B1, April 23, 2002.
9. A. Dieng, J.C. Le Claire, M.F. Benkhoris and M. Ait-Ahmed, "*Control of Single-phase Double Boost Effect AC-DC Converter*", Journal of Electrical Engineering, JEE, Vol. 14, Edition 3, pp. 1-9, 2014.
10. N. GINOT, "*Etude et conception d'un onduleur modulaire exploitant une structure multi-convertisseurs pour obtenir une haute dynamique*", PhD thesis, University of Nantes, Novembre 2004.
11. J.C. Le Claire, "*Power Electronic Converters – PWM Strategies and Current Control Techniques*", Chapter 14, "*Current Control Using Self-Oscillating Current Controllers*", ISTE, London, UK, 2011, WILEY, Hoboken, USA, 2011, pp 417-447.